




 Cite this: *RSC Adv.*, 2021, **11**, 2608

# Selection and characterization of toxic *Aspergillus* spore-specific DNA aptamer using spore-SELEX

 Jin-Woo Seo,<sup>a</sup> Jee Young Kim,<sup>a</sup> Da Hee Kim,<sup>a</sup> Jeong-Joo Oh,<sup>a</sup> Young Jun Kim <sup>b</sup> and Gyu-Hyeok Kim <sup>\*a</sup>

As airborne spores of toxic *Aspergillus* species cause mild symptoms to invasive fungal infections, their indoor concentration should be controlled through real-time management. Aptamer-based biosensors could provide economical and simple solutions for point-of-care. In this study, we isolated aptamers binding to the spores of three representative toxic *Aspergillus* species (*A. fumigatus*, *A. flavus*, and *A. niger*) for the first time, using cell-SELEX (systematic evolution of ligands through exponential enrichment). Among the aptamer candidates, Asp-3 showed a broad and high binding affinity for the *Aspergillus* spores. Considering the low binding affinity with proteinase-treated spores, we speculated that the Asp-3 binding sites could be possibly associated with cell surface proteins. The high Asp-3 specificity was confirmed by comparing the binding affinity between the *Aspergillus* target species and other common indoor fungal species. Moreover, we also established quantitative linear relationships between Asp-3 and the spore concentration of each *Aspergillus* species. Therefore, the selected Asp-3 aptamer, conjugated with detection sensors, could be an effective biorecognition element for the spores of three toxic *Aspergillus* species.

 Received 11th November 2020  
 Accepted 28th December 2020

DOI: 10.1039/d0ra09571k

[rsc.li/rsc-advances](http://rsc.li/rsc-advances)

## 1. Introduction

As modern people spend most of their time indoors, long-term exposure to indoor air significantly affects health.<sup>1</sup> Among the various indoor contaminants, molds, especially airborne fungal spores, are significant fungal aerosol contaminants.<sup>2–5</sup> Low concentrations of indoor fungal spores are barely associated with ill health. However, elevated fungal spore concentrations could adversely affect health, especially upper-respiratory allergic reactions induced by fungal cell wall materials.<sup>3–6</sup> Such undesirable indoor air conditions could lead not only to mild symptoms but also invasive fungal infections (IFIs).<sup>7,8</sup> In immunocompromised individuals, the inhalation of pathogenic fungal spores could induce respiratory IFIs. In severe cases, fungi spread to each part of the body, which may even cause death.<sup>9</sup> Among fungi, the genus *Aspergillus* is one of the most commonly observed indoor species.<sup>7,8</sup> *Aspergillus* spp. superbly adapt their spores to airborne dissemination, and each fruiting body could generate approximately 10 000 spores.<sup>10</sup> Previous studies have reported that inhaling airborne *Aspergillus* spores can directly cause lung infection.<sup>8,10,11</sup> For example, *A. fumigatus*, with small size (3–5 μm) spores, could penetrate deeply into the host lung due to the hydrophobic protein-coat

layer of its spores.<sup>7</sup> In addition, aspergillosis, the most common fungal disease caused by *Aspergillus* spp., could lead to a mortality rate of over 50% among the immunocompromised patients, even with proper diagnosis and treatment.<sup>11,12</sup> Due to these risks, *Aspergillus* spp. spores are in the focus of scientific attention.<sup>10</sup> A rapid diagnostic assay could be considered a reasonable solution as the direct evaluation of the spores could establish proper guidelines to effectively manage *Aspergillus* airborne spores.<sup>13</sup>

Air sampling is a commonly used method in various diagnostic assays to assess indoor fungal spore contamination.<sup>13</sup> These conventional laboratory-based methods for air sample diagnosis assays rely on a culture of sampled fungi.<sup>14,15</sup> Although culture-based methods are advantageous for sample maintenance to facilitate the in-depth identification of fungi, they are time-consuming and laborious, and it is hard to cultivate all collected microorganisms using such methods, which requires equipment with specialized laboratories.<sup>16</sup> Apart from the culture-based methods, studies of advanced analytical techniques combined with commercial air samplers have been recently conducted. For instance, quantitative polymerase chain reaction (qPCR) and Luminex xMAP techniques were combined with an air sampler and used for the identification of fungi in the air.<sup>17,18</sup> However, even with such advanced supersensitive sensor-based methods, there still remain few drawbacks, such as high equipment cost and need for highly skilled personnel, making it hard to use such approaches as effective “point-of-care” management systems.

<sup>a</sup>Division of Environmental Science & Ecological Engineering, College of Life Sciences & Biotechnology, Korea University, 145, Anam-ro, Seongbuk-gu, Seoul 02841, Korea. E-mail: lovewood@korea.ac.kr; Fax: +82 2 3290 9753; Tel: +82 2 3290 3014

<sup>b</sup>Life Science and Biotechnology Department, Underwood Division, Underwood International College, Yonsei University, Seoul, 03722, Korea



Alternatively, aptamers, single-stranded oligonucleotide (DNA or RNA) molecules that bind to other molecules with high affinity and specificity, are becoming attractive elements for various types of sensors due to their high stability, low production cost, and ease of modification compared to other biorecognition elements (*e.g.*, enzymes, antibodies, and lectin).<sup>19–21</sup> These advantages allow the easy generation of target-specific aptamers *in vitro*, under the same conditions as those used for detection, which is a clear advantage compared to other sensor elements.<sup>22,23</sup> Therefore, sensors aptamer-based could be used as “lab-on-a-chip” tools without specialized personnel and establishing a full laboratory system.<sup>24</sup>

The procedure for selecting a target-specific aptamer, the systematic evolution of ligands through exponential enrichment (SELEX), was developed, in 1990, by Gold and Szostak.<sup>25,26</sup> Over the years, various SELEX methods have been developed to suit the needs of the researchers. Among these variations, cell-SELEX is a promising method for the identification of aptamers on the cell membrane surface without prior knowledge of the target.<sup>27</sup> Several aptamers have been selected using cell-SELEX that are conjugated to optical, mechanical, and electrochemical biosensors to overcome the problems of traditional pathogen detection methods.<sup>28,29</sup> However, no aptamers isolated from fungal spore cell-SELEX have been reported, whereas fungal element-targeting aptamers, such as fungal toxins and cell wall components, have been explored.<sup>28,30,31</sup>

In this study, based on cell-SELEX, we performed spore-SELEX to isolate broadly reactive aptamers binding to the spores of three representative *Aspergillus* species (*A. fumigatus*, *A. flavus*, and *A. niger*), generating large amounts of airborne fungal spores that subsequently cause allergic reactions and even IFIs.<sup>7,8</sup> After 12 rounds of SELEX, we successfully isolated *Aspergillus* spore-specific aptamer candidates. Asp-3 was selected post-SELEX as the most efficient aptamer. Thereafter, we evaluated the Asp-3 binding affinity and specificity to the spores of the three toxic *Aspergillus* target species. This study provides basic information on aptamer binding to fungal spores for the development of highly sensitive biosensors, offering a solution for indoor air quality management.

## 2. Results and discussion

### 2.1. Spore-SELEX against spores of three *Aspergillus* spp.

Spore-SELEX was conducted to isolate *Aspergillus* spore-specific aptamers. Spore-SELEX is used to isolate aptamers with a broad affinity for various microorganisms, by performing cell-SELEX at different targets of interest in each round of aptamer selection.<sup>32</sup> Fig. 1 illustrates the spore-SELEX procedure performed in this study. Starting with a random single-stranded DNA (ssDNA) library, 12 rounds ( $3 \times 4$  cycles, each consisting of three *Aspergillus* species SELEX procedure in regular sequence) of positive selection were performed with each spore suspension of *A. fumigatus*, *A. flavus*, and *A. niger*. Moreover, two steps

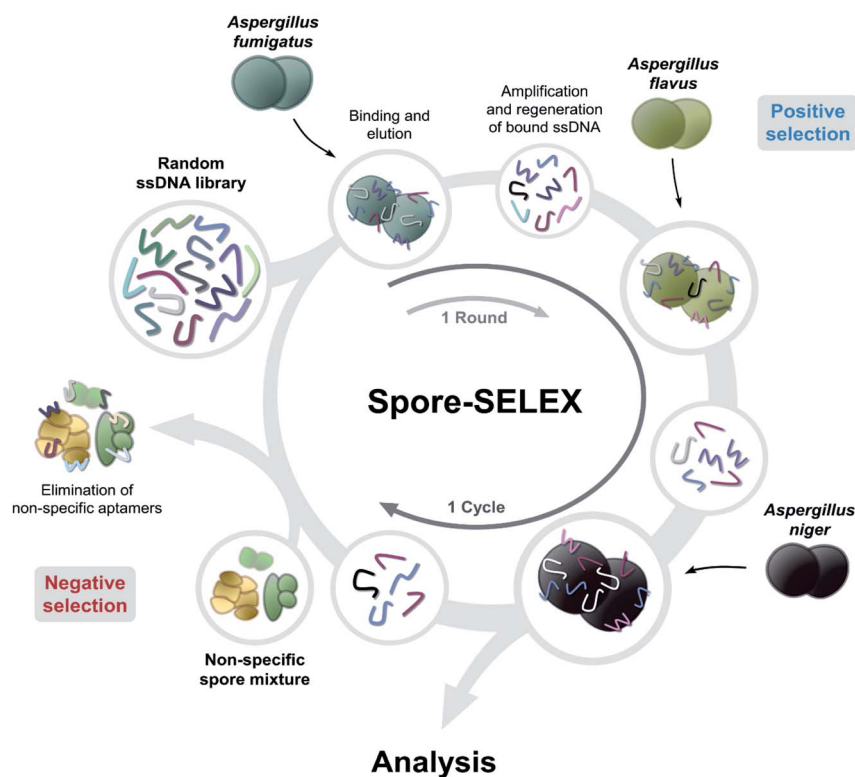


Fig. 1 Schematic illustration of strategies exploited for selecting aptamers binding to the spores of three toxic *Aspergillus* species. Starting from random ssDNA library, 4 cycles of 3 rounds (total 12 rounds) sequential positive selections (*A. fumigatus*, *A. flavus*, and *A. niger*) were performed. Negative selections with non-specific spore mixtures were performed at rounds 4 and 7 to eliminate non-specific aptamers.



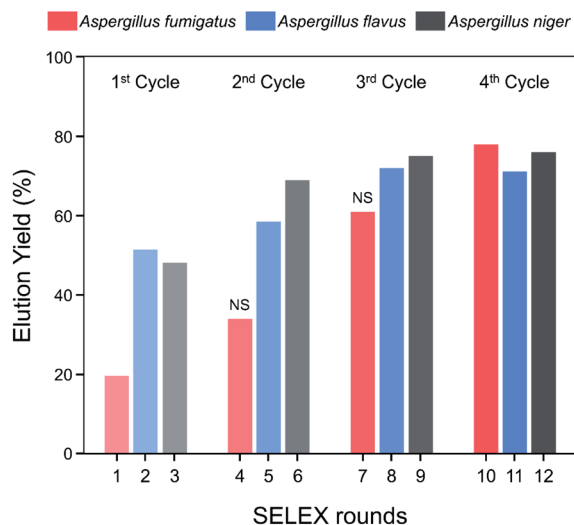


Fig. 2 Elution yield of ssDNA at each round of the spore-SELEX procedure. Before rounds 4 and 7, NS (negative selection) was performed to removed non-specific aptamers.

of negative selection were conducted just before rounds 4 and 7 with non-specific spore suspensions of *Alternaria alternata*, *Cladosporium cladosporioides*, and *Penicillium chrysogenum*, respectively.

The elution yields (%) of each round during the spore-SELEX are illustrated in Fig. 2. This elution yield (%) showed a gradual increase from the 1<sup>st</sup> to the 4<sup>th</sup> cycle during the SELEX procedure. The final yield of the 4<sup>th</sup> cycle was saturated near 70–80%. These results suggest that repetitive SELEX cycles reduce the amount of unnecessary nucleotides and enable us to obtain a broad affinity for aptamers against the spores of the three toxic *Aspergillus* species. The saturation of the elution yield at the 4<sup>th</sup> cycle was likely caused by the bottleneck effect from decreasing the variety of the aptamer candidates and consequently the saturation of the binding sites, indicating that 4 cycles were optimal for the SELEX procedure with no need for further rounds. In addition, the reduction of the elution yield at round 4 (48.1–34.0%) and round 7 (69.0–61.0%) showed that the negative selection was successfully applied to remove non-specifically bound aptamers from the aptamer candidates and enhance the target

specificity of the selected aptamer. Finally, the aptamer pool obtained after round 12 was selected and identified using TA cloning and subsequent DNA sequencing.

A total of 20 clones were sequenced and 8 different sequences (71-nt) were obtained (Table 1). From 8 different sequences, Asp-3, Asp-5, Asp-6, Asp-7, and Asp-8 were chosen as aptamer candidates, based on their Gibbs free energy and the number of copies. The five aptamer candidates had the lowest Gibbs free energy, among which Asp-3 and Asp-5 had a number of copies of at least 2. The 2D structure and Gibbs free energy of the five aptamer candidates are illustrated in Fig. 3A. All five aptamer candidates showed more than three bulb-like hairpin structures.

## 2.2. Post-SELEX of aptamer candidates

The post-SELEX experiment was conducted to select the most efficient binding aptamers to the spores of the three *Aspergillus* species. Fig. 3B shows the fluorescence intensity of each spore-bound aptamer candidate, Asp-3 displaying the highest binding affinity. The average fluorescence intensity of the spore-bound Asp-3 and Asp-8 aptamers were 10 and 8 times higher than those of the random ssDNA library, respectively. The Asp-7 aptamer showed noticeable binding affinity only against *A. fumigatus* and *A. niger*, which was unsuitable for simultaneous detection of the spores of the three *Aspergillus* species. The binding affinity of Asp-5 and Asp-6 was not as high as those of Asp-3 and Asp-8, possibly due to their binding with fungal elements, such as secondary metabolites, other than spores. Based on its broad and high binding affinity, aptamer Asp-3 was finally designated as the most efficient binding aptamer to the spores of the three *Aspergillus* species, and further analysis was conducted for its characterization.

## 2.3. Asp-3 binding assay and binding site identification on the spores

Binding saturation curves were plotted to calculate the Asp-3 dissociation constant ( $K_d$ ) to the spores of the three *Aspergillus* species. The binding saturation curves were fitted using the following formula:

$$\text{Michaelis-Menten equation: } F = B_{\max} \times C / (K_d + C), \quad (1)$$

Table 1 Sequenced ssDNA from 4<sup>th</sup> cycle of spore-SELEX procedure

| ID    | Random region                         | Number of copies | Gibbs free energy (kcal mol <sup>-1</sup> ) |
|-------|---------------------------------------|------------------|---|
| Asp-1 | ttaggtttaaaggcgagaataattaaagattta     | 1                | −6.65                                       |
| Asp-2 | ggtgctctgctgggtggcttgatggtattgctt     | 1                | −7.47                                       |
| Asp-3 | cgttggcggtatgagttcgggggtataccgcag     | 2                | −11.86                                      |
| Asp-4 | atgttttgtcttttggcttacaggaatgggtgt     | 1                | −6.67                                       |
| Asp-5 | tgecttaagtgggtgctctcggattcctagtgtat   | 12               | −11.38                                      |
| Asp-6 | tcgtgctcttagtgagaaaggcctcggctacagc    | 1                | −8.34                                       |
| Asp-7 | cggggtgagactcttgaaggaacgaggtccatag    | 1                | −15.37                                      |
| Asp-8 | tgectctaggttggtgctcctcggattcctagtgtat | 1                | −10.23                                      |



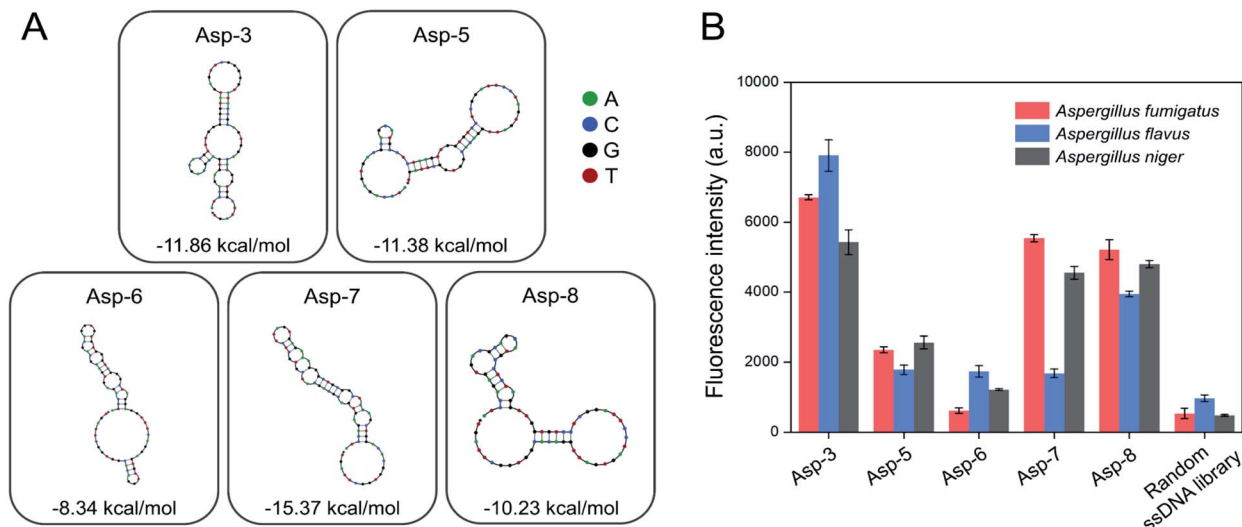


Fig. 3 Selection of nucleotides binding to the spores of three toxic *Aspergillus* species from the enriched pool after the 4<sup>th</sup> toggle (A) secondary structure and Gibbs free energy ( $\Delta G$ , kcal mol<sup>-1</sup>) predictions of five aptamer candidates based on the NUPACK software analysis (B) binding affinity of five aptamer candidates to the spores of three toxic *Aspergillus* species based on fluorescence intensity.

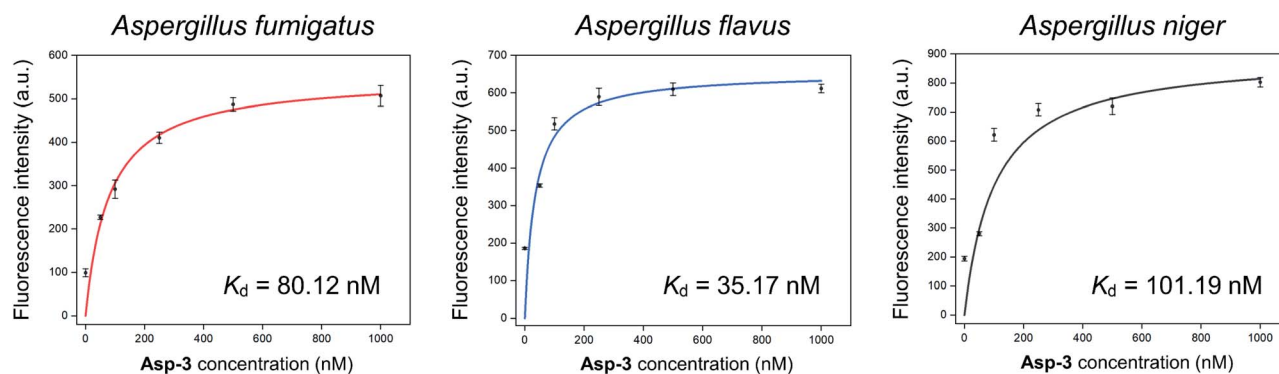


Fig. 4 Binding saturation curves of the Asp-3 aptamer to the spores of three toxic *Aspergillus* species based on fluorescence intensity.

where  $F$ ,  $B_{\max}$ , and  $C$  (nM) are the fluorescence intensity, maximum fluorescence intensity of binding, and aptamer concentration, respectively.

The calculated Asp-3  $K_d$  was  $80.12 \pm 7.01$ ,  $35.17 \pm 12.11$ , and  $101.19 \pm 25.41$  nM to the spores of *A. fumigatus*, *A. flavus*, and *A. niger*, respectively (Fig. 4). Among the spores, the Asp-3 binding affinities were in the following order: *A. flavus*, *A. fumigatus*, and *A. niger*. Overall, these  $K_d$  values are comparable to those of isolated aptamers to fungal elements in the cell wall. Aptamers with an affinity for fungal cell wall components, such as (1 $\rightarrow$ 3)- $\beta$ -D-glucan, showed  $K_d$  between 79.76 nM and 103.7 nM.<sup>33</sup> Since cell-SELEX is a method for identifying new biomarkers on the cell membrane surface, these comparable binding affinities show that Asp-3 could recognize surface molecules on the spores with high affinity.

In order to identify the Asp-3 target molecules, the spores of each *Aspergillus* species were treated with two types of proteinases. Fig. 5 shows proteinase-treated and -untreated spore-bound Asp-3 fluorescence intensity of the three toxic

*Aspergillus* species. The intensities of trypsin- and proteinase K-treated spores were significantly lower than those of the untreated spores of all three *Aspergillus* species. These results indicate that each type of the *Aspergillus* spores shares similar binding sites and is most likely a spore surface protein. For reference, outer layers of *Aspergillus* spores are mainly composed of hydrophobic proteins called hydrophobins.<sup>34</sup> As many *Aspergillus* species display various types of putative hydrophobins on their spore surfaces, the SELEX-isolated aptamer might target the major types of *Aspergillus* hydrophobins.<sup>34,35</sup>

#### 2.4. Asp-3 specificity evaluation

Spore mixtures of the three fungal species (*Al. alternata*, *C. cladosporioides*, and *P. chrysogenum*) were used as negative selection samples for the SELEX as the selected aptamers should be non-specific to other common indoor fungi for application to environmental samples.<sup>36</sup> To confirm the specificity of the Asp-3 aptamer, the binding affinity of Asp-3 was





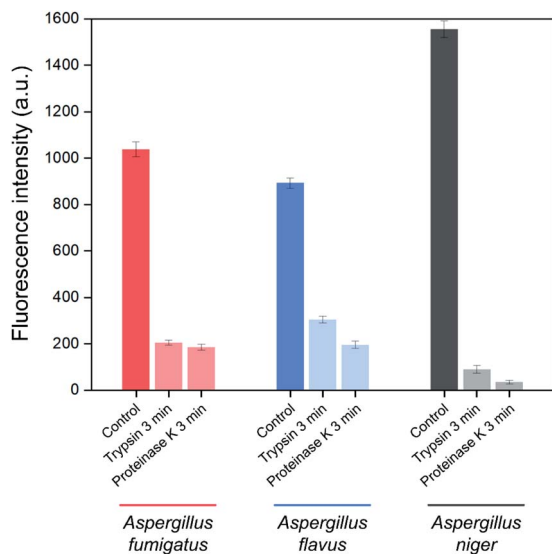


Fig. 5 Effect of trypsin and proteinase K treatments on the binding affinity of Asp-3 aptamer to the spores of three toxic *Aspergillus* species based on fluorescence intensity.

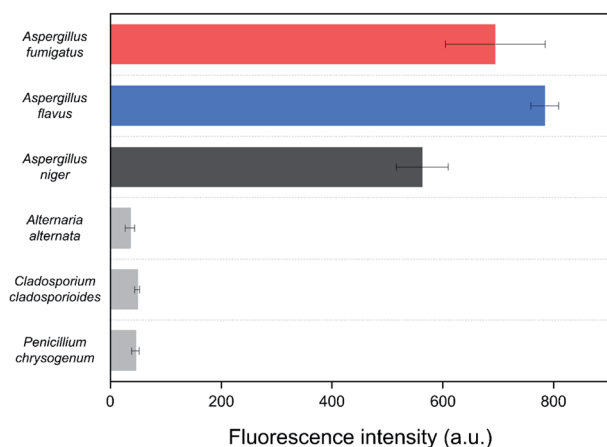


Fig. 6 Binding affinity of Asp-3 aptamer to the spores of three toxic *Aspergillus* species and three common indoor fungal species, *Al. alternata*, *C. cladosporioides*, and *P. chrysogenum* based on fluorescence intensity.

evaluated with each spore suspension of common fungal species. Fig. 6 shows the fluorescent intensity of Asp-3 binding to spores of three common indoor fungi and three toxic *Aspergillus* spp. Significant differences in fluorescence intensity were observed between spores of target *Aspergillus* species and other fungal species. The average intensities of Asp-3 binding with *Aspergillus* spores were 16 times higher than those of other fungal spores. These results indicate a successful spore-SELEX procedure and the noticeable specificity of Asp-3, suggesting a potential application of Asp-3 in detecting specific *Aspergillus* species in an indoor environment.

### 2.5. Asp-3-based quantification of the spore concentration

The quantification of the spores of the three *Aspergillus* species was confirmed using Asp-3. Fig. 7 shows the normalized signals  $((F - F_0)/F_0)$  of Asp-3 bound to different concentrations ( $5 \times 10^5$ ,  $10^6$ ,  $1.5 \times 10^6$ ,  $2 \times 10^6$ ,  $5 \times 10^6$ ,  $1 \times 10^7$  spores per mL) of *Aspergillus* target spores. The normalized signals were visibly proportional to the concentration of the target spores. Then, these data points were fitted to a linear relationship, using the following formulas:

$$A. \text{ fumigatus: } f(x) = 3.40 \times 10^{-5}x \quad (R^2 = 0.95), \quad (2)$$

$$A. \text{ flavus: } f(x) = 5.66 \times 10^{-5}x \quad (R^2 = 0.97), \quad (3)$$

$$\text{and } A. \text{ niger: } f(x) = 2.12 \times 10^{-5}x \quad (R^2 = 0.98), \quad (4)$$

where  $f(x)$  and  $x$  (spores per mL) are the normalized signal and spore concentrations of the target *Aspergillus* species, respectively.

The coefficients of the fitted model determinations were higher than 0.95, indicating that the models were highly accurate in quantifying each *Aspergillus* spore concentration. Further research is necessary to apply the selected aptamer (Asp-3) for monitoring of airborne spores of *Aspergillus* species via combining it with various sensing platforms such as gold nanoparticles, paper strips, and surface plasmon resonance.<sup>36–38</sup>

## 3. Conclusion

In summary, the spore-SELEX method was successfully used to isolate Asp-3, an aptamer with broad and high binding affinity

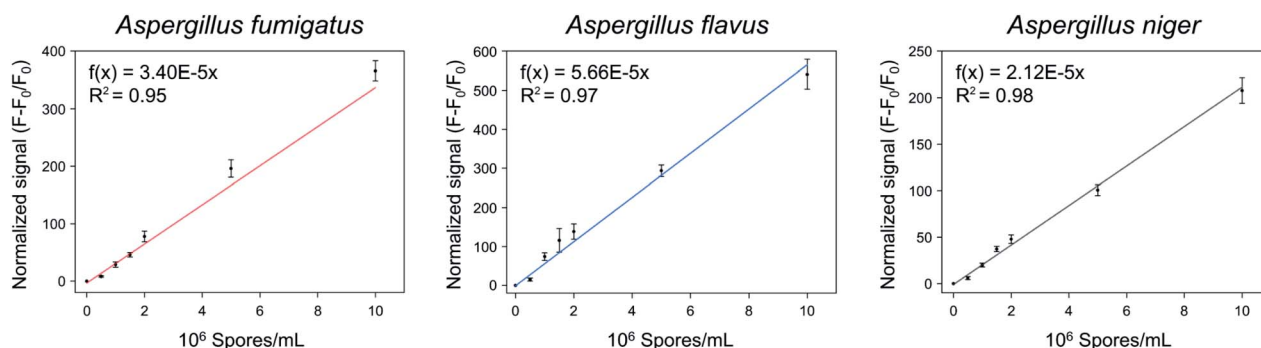


Fig. 7 Quantitative analysis of the spores of three toxic *Aspergillus* species using Asp-3 based on fluorescence intensity.



for the spores of three toxic *Aspergillus* species. Each  $K_d$  against *A. fumigatus*, *A. flavus*, and *A. niger* were 80.12, 35.17, and 101.19 nM, respectively. The Asp-3 binding sites on the spore surface were possibly associated with cell surface proteins. The high Asp-3 specificity was confirmed by comparing the binding affinity between the target *Aspergillus* and other fungal species. The quantitative linear relationships between Asp-3 and the *Aspergillus* spore concentrations were also established. Therefore, this identified aptamer, Asp-3, could be a potential candidate conjugated with sensors to detect the spores of three toxic *Aspergillus* species.

## 4. Materials and methods

### 4.1. Materials

Phosphate-buffered saline (PBS, pH = 7.0), bovine serum albumin (BSA),  $MgCl_2$ , NaOH, EDTA, and trypsin were purchased from Sigma-Aldrich (St. Louis, MO, USA). Potato Dextrose Agar (PDA) was purchased from BD (MD, USA). Tween® 80 was purchased from Junsi Chemical (Tokyo, Japan). Distilled water (DNase-free), salmon sperm DNA, and streptavidin-coupled magnetic beads were purchased from Invitrogen Corporation (Karlsruhe, Germany). The *AccuPrep* Gel Purification kit, proteinase K, and the 50× Tris-acetate-EDTA (TAE) buffer were purchased from Bioneer (Daejeon, Korea). The PCR premix was purchased from Cellsafe (Gyeonggi, Korea). The random single-strand DNA (ssDNA) library and primers used in *Aspergillus* spore-SELEX were chemically synthesized by Integrated DNA Technologies (Coralville, IA, USA). The library sequence combination of 71-nucleotides (nt) is composed of a 35-nt randomized region flanked by primers (5'-ATCCAGAGTGACGCAGCA-[N]<sub>35</sub>-TGGACACGGTGGCTTAGT-3') on both sides. The fungal spore-bound probes obtained from the SELEX process were PCR-amplified using the following primers: forward primer (5'-ATC-CAGAGTGACGCAGCA-3') and biotinylated reverse primer (5'-biotin-ACTAAGCCACCGTGTCCA-3').<sup>27</sup>

### 4.2. Fungal strains

*A. flavus* var. *columnaris* (KCTC 6603), *A. fumigatus* (KCTC 6145), *A. niger* (KCTC 6960), and *Al. alternata* (KCTC 26781), as well as *C. cladosporioides* (KCTC 26799) and *P. chrysogenum* (KCTC 6444), were obtained from the Korean Collection for Type Culture (KCTC, Jeongeup-si, Korea). All fungal strains were cultured on nutrient agar (39.0 g of PDA in 1 L of distilled water) at 30 °C under aerobic conditions. A spore suspension of each fungal species was prepared by scraping spores from the fungal medium using 0.02% Tween® 80 surfactant and washed three times with PBS, then resuspended ( $10^6$  spores per mL) before subsequent use for the experiments.

### 4.3. Spore-SELEX process

A total of 12 rounds consisting of 4 cycles of 3 rounds sequential positive selection (*A. fumigatus*, *A. flavus*, and *A. niger*) was performed. Negative selection with non-specific spore mixtures (*Al. alternata*, *C. cladosporioides*, and *P. chrysogenum*), was performed at rounds 4 and 7 (Fig. 1).<sup>32</sup> Each round of SELEX

consisted of three steps as follows: binding and elution, PCR amplification, and ssDNA recovery.

In the first round of selection, the initial random ssDNA library (100 pmol) was mixed in the binding buffer (PBS containing 1.4 mM  $MgCl_2$ , 1  $\mu g \mu L^{-1}$  BSA, and 1  $\mu g \mu L^{-1}$  salmon sperm DNA) and heated at 95 °C for 5 min, followed by ice-cooling for proper folding of the aptamer structures.<sup>39,40</sup> The random ssDNA aptamer pool, mixed in the binding buffer, was incubated with 1 mL of *Aspergillus* spore suspension. The mixture was incubated at 21 °C for 30 min with gentle shaking in order to allow the successful binding of the spores and the ssDNA. The unbound ssDNA that remained in the supernatant was discarded by washing with 1 mL of PBS three times and once with distilled water after centrifugation at 4618g for 5 min. To elute the *Aspergillus* spore-bound ssDNA, spore pellets were resuspended in 100  $\mu L$  of distilled water and heated at 95 °C for 10 min to detach the ssDNA from the spores and then immediately placed on ice for 10 min. The eluted ssDNA in the supernatant was recovered using centrifugation (4618g) for 5 min, and then purified using overnight ethanol precipitation. After purification, the ssDNA was resuspended in 100  $\mu L$  of distilled water and the elution yield was calculated by comparing the amount of ssDNA before and after binding to the *Aspergillus* spores using a Nanodrop spectrophotometer (Colibri LB 915, JC Bio, Seoul, Korea). In order to obtain an aptamer of high specificity, we gradually increased the selection pressure by decreasing the input amount of ssDNA. The negative selection was performed immediately after the 1<sup>st</sup> and 2<sup>nd</sup> cycles to ensure aptamer specificity to the candidates. For negative selection, the aptamer pool from the previous round was added to a non-specific cell mixture (1 mL of *Al. alternata*, *C. cladosporioides*, and *P. chrysogenum* spore suspensions ( $1 \times 10^6$  spores per mL)) and incubated at 21 °C for 30 min with gentle shaking. The non-specific cell-bound ssDNA was then discarded, while unbound ssDNA in the supernatant was used for the next round of positive selection.

PCR was performed to amplify the recovered ssDNA from the above-mentioned procedure by using a pair of forward and modified reverse primers, as well as a PCR premix. The PCR conditions were as follows: an initial step of denaturation for 150 s at 95 °C, followed by 10 cycles of denaturation at 95 °C for 30 s, annealing at 56.3 °C for 30 s, extension at 72 °C for 30 s, and final extension for 3 min at 72 °C. After amplification, the concentration and size of the PCR amplicons were confirmed by gel electrophoresis on a 2% agarose gel in TAE buffer at 100 V for 20 min and subsequent purification using the gel purification kit according to the manufacturer's recommendation.

The ssDNA was recovered from double-stranded DNA (dsDNA) PCR amplicons using streptavidin-coupled magnetic beads. The PCR amplicons were incubated in the streptavidin-coated magnetic bead-containing solution for 30 min at 21 °C. After 30 min of incubation, the beads were subjected to magnetic separation and washed three times with PBS. Then, the beads were incubated in 500  $\mu L$  of NaOH (200 mM) for 10 min at 21 °C. The supernatant was then recovered, followed by concentration and purification using 3 K centrifugal filters (Merck, Burlington, MA). The recovered ssDNA was quantified



using a Nanodrop spectrophotometer and used for the next round of SELEX. After the binding and elution steps of the last round, the recovered ssDNA was amplified using a pair of forward and non-modified reverse primers and purified as mentioned previously. The purified PCR amplicons of the last round were then cloned and sequenced by Macrogen (Seoul, Korea).

#### 4.4. Cloning and post-SELEX

A total of 8 different sequences were obtained by analyzing 20 clones. Five aptamer candidates (Asp-3, Asp-5, Asp-6, Asp-7, and Asp-8) were chosen as post-SELEX candidates because of their potential high affinity based on their multiple overlapping sequences and Gibbs free energy. The secondary structures of the selected sequences were predicted with the Gibbs free energy minimization algorithm using the nucleic acid package (NUPACK) software, then grouped according to their similarities.<sup>41</sup> In order to further confirm their binding affinities, five aptamer candidates were labeled with 6-carboxyfluorescein (FAM) at their 5' end and synthesized (Integrated DNA Technologies). An aliquot of 500 nM of the five aptamer candidates was dissolved in 100  $\mu$ L of binding buffer mixed with 1 mL of the three *Aspergillus* spore suspensions ( $1 \times 10^6$  spores per mL), and incubated for 30 min with gentle shaking at 21  $^{\circ}$ C. The supernatants were then discarded by washing with 1 mL of PBS three times after centrifugation at 4618g for 5 min. After washing, spore pellets were resuspended in 100  $\mu$ L of distilled water and heated at 95  $^{\circ}$ C for 10 min to detach the aptamer from the spores, then ice-cooled for 10 min. The eluted aptamers were recovered in the supernatant using centrifugation (4618g). The mixtures were then moved to a 96-well black microplate (SPL, Gyeonggi, Korea) to measure their fluorescence intensities using a SpectraMax i3 Multi-Mode Platform (Molecular Devices, San Jose, CA) under 490 and 530 nm excitation and emission wavelengths, respectively.

#### 4.5. Measurement of the disassociation constant ( $K_d$ )

We performed the characterization of the selected Asp-3 aptamer on the spores of the three *Aspergillus* species using the same methods and conditions for the binding and elution steps as described previously. To measure the  $K_d$  of Asp-3 for the three *Aspergillus* target spores, 1 mL of each spore suspension of the three *Aspergillus* ( $1 \times 10^6$  spores per mL) species and various concentrations (0, 50, 100, 250, 500, and 1000 nM) of the Asp-3 aptamer were mixed in the binding buffer and incubated for 30 min with gentle shaking at 21  $^{\circ}$ C. After incubation, we washed and eluted the samples, then measured the fluorescence intensity of the mixtures as described above. The  $K_d$  of Asp-3 for each *Aspergillus* spore sample was calculated according to nonlinear regression analysis. The  $K_d$  measurement was performed in triplicates.

#### 4.6. Identification of selected aptamer binding sites on the spores

To verify the Asp-3 binding site on the three *Aspergillus* target spores, 1 mL of spore suspension of each *Aspergillus* ( $1 \times 10^6$

spore per mL) sample was incubated with 0.05% of trypsin/0.53 mM EDTA and 0.1 mg mL<sup>-1</sup> of proteinase K for 3 min at 37  $^{\circ}$ C.<sup>42</sup> After washing, the treated spores were incubated with 1 mM of Asp-3 dissolved in 100  $\mu$ L of binding buffer for 30 min at 21  $^{\circ}$ C, followed by washing and elution. Finally, the fluorescence intensity of the mixture was measured in triplicates as described above.

#### 4.7. Specificity assay

In order to measure Asp-3 sensitivity and specificity, its binding affinity to positive (*A. fumigatus*, *A. flavus*, and *A. niger*) and negative (*Al. alternata*, *C. cladosporioides*, and *P. chrysogenum*) selection strains was evaluated. The spore suspension of each fungal species ( $1 \times 10^6$  spores per mL) was tested using 1 mM of Asp-3 dissolved in 100  $\mu$ L of binding buffer. This mixture was then incubated for 30 min with gentle shaking at 21  $^{\circ}$ C. After incubation, washing, and elution, the fluorescence intensity of the mixtures was measured as described above.

## Conflicts of interest

There are no conflicts to declare.

## Acknowledgements

This study was supported by a Korea University Research Grant.

## References

- 1 J. Sundell, *Indoor Air*, 2004, **14**, 51–58.
- 2 X. Wang, W. Liu, C. Huang, J. Cai, L. Shen, Z. Zou, R. Lu, J. Chang, X. Wei and C. Sun, *Build. Environ.*, 2016, **102**, 159–166.
- 3 M. J. Mendell, A. G. Mirer, K. Cheung, M. Tong and J. Douwes, *Environ. Health Perspect.*, 2011, **119**, 748–756.
- 4 M. H. Garrett, P. R. Rayment, M. A. Hooper, M. J. Abramson and B. M. Hooper, *Clin. Exp. Allergy*, 1998, **28**, 459–467.
- 5 D. M. Kuhn and M. A. Ghannoum, *Clin. Microbiol. Rev.*, 2003, **16**, 144–172.
- 6 F. Fung and W. G. Hughson, *Appl. Occup. Environ. Hyg.*, 2003, **18**, 535–544.
- 7 D. W. Denning, *Clin. Infect. Dis.*, 1998, 781–803.
- 8 J. P. Latge and G. Chamilos, *Clin. Microbiol. Rev.*, 2019, **33**, e00140-18.
- 9 S. Metcalf and D. Dockrell, *J. Infect.*, 2007, **55**, 287–299.
- 10 F. S. Rhame, *J. Hosp. Infect.*, 1991, **18**, 466–472.
- 11 A. A. Brakhage, *Curr. Drug Targets*, 2005, **6**, 875–886.
- 12 H. S. Nam, K. Jeon, S. W. Um, G. Y. Suh, M. P. Chung, H. Kim, O. J. Kwon and W. J. Koh, *Int. J. Infect. Dis.*, 2010, **14**, e479–e482.
- 13 X. Li, X. Zhang, Q. Liu, W. Zhao, S. Liu and G. Sui, *ACS Sens.*, 2018, **3**, 2095–2103.
- 14 T. Lee, S. A. Grinshpun, D. Martuzevicius, A. Adhikari, C. M. Crawford and T. Reponen, *Atmos. Environ.*, 2006, **40**, 2902–2910.



- 15 J. H. Jin, J. Kim, T. Jeon, S. K. Shin, J. R. Sohn, H. Yi and B. Y. Lee, *RSC Adv.*, 2015, **5**, 15728–15735.
- 16 D. Petinataud, S. Berger, C. Ferdynus, A. Debourgogne, N. Contet-Audonneau and M. Machouart, *Mycoses*, 2016, **59**, 304–311.
- 17 J. B. Emerson, P. B. Keady, T. E. Brewer, N. Clements, E. E. Morgan, J. Awerbuch, S. L. Miller and N. Fierer, *Environ. Sci. Technol.*, 2015, **49**, 2675–2684.
- 18 K. Kostov, E. Verstappen, J. Bergervoet, M. De Weerd, C. Schoen, S. Slavov and P. Bonants, *Plant Pathol.*, 2016, **65**, 1008–1021.
- 19 S. H. Kim, T. T. T. Thoa and M. B. Gu, *Curr. Opin. Environ. Sci. Health*, 2019, **10**, 9–21.
- 20 S. Song, L. Wang, J. Li, C. Fan and J. Zhao, *TrAC, Trends Anal. Chem.*, 2008, **27**, 108–117.
- 21 M. Yüce and H. Kurt, *RSC Adv.*, 2017, **7**, 49386–49403.
- 22 M. Saad, D. Chinerman, M. Tabrizian and S. P. Faucher, *Sci. Rep.*, 2020, **10**, 1–10.
- 23 M. Jarczewska, Ł. Górski and E. Malinowska, *Anal. Methods*, 2016, **8**, 3861–3877.
- 24 A. Ahmed, J. V. Rushworth, N. A. Hirst and P. A. Millner, *Clin. Microbiol. Rev.*, 2014, **27**, 631–646.
- 25 A. D. Ellington and J. W. Szostak, *Nature*, 1990, **346**, 818–822.
- 26 C. Tuerk and L. Gold, *Science*, 1990, **249**, 505–510.
- 27 K. Sefah, D. Shangguan, X. Xiong, M. B. O'donoghue and W. Tan, *Nat. Protoc.*, 2010, **5**, 1169.
- 28 H. Kaur, *Biochim. Biophys. Acta, Gen. Subj.*, 2018, **1862**, 2323–2329.
- 29 J. Barman, *RSC Adv.*, 2015, **5**, 11724–11732.
- 30 N. Alizadeh, M. Memar, B. Mehramuz, S. Abibiglou, F. Hemmati and H. Samadi Kafil, *J. Appl. Microbiol.*, 2018, **124**, 644–651.
- 31 Z. Lu, X. Chen, Y. Wang, X. Zheng and C. M. Li, *Microchim. Acta*, 2015, **182**, 571–578.
- 32 M. Y. Song, D. Nguyen, S. W. Hong and B. C. Kim, *Sci. Rep.*, 2017, **7**, 43641.
- 33 X. L. Tang, Y. Hua, Q. Guan and C. H. Yuan, *Eur. J. Clin. Microbiol. Infect. Dis.*, 2016, **35**, 587–595.
- 34 R. Garcia-Rubio, H. C. de Oliveira, J. Rivera and N. Trevijano-Contador, *Front. Microbiol.*, 2020, **10**, 2993.
- 35 M. Bernard and J. P. Latgé, *Med. Mycol.*, 2001, **39**, 9–17.
- 36 W. R. Shin, S. S. Sekhon, S. G. Kim, S. J. Rhee, G. N. Yang, K. Won, S. K. Rhee, H. Ryu, K. Kim and J. Min, *J. Biomed. Nanotechnol.*, 2018, **14**, 1992–2002.
- 37 Y. C. Chang, C. Y. Yang, R. L. Sun, Y. F. Cheng, W. C. Kao and P. C. Yang, *Sci. Rep.*, 2013, **3**, 1–7.
- 38 W. R. Shin, S. S. Sekhon, S. K. Rhee, J. H. Ko, J. Y. Ahn, J. Min and Y. H. Kim, *ACS Comb. Sci.*, 2018, **20**, 261–268.
- 39 G. Mayer, M. S. L. Ahmed, A. Dolf, E. Endl, P. A. Knolle and M. Famulok, *Nat. Protoc.*, 2010, **5**, 1993–2004.
- 40 J. Y. Kim, J. J. Oh, D. H. Kim, J. Park, H. S. Kim and Y. E. Choi, *J. Agric. Food Chem.*, 2019, **68**, 402–408.
- 41 J. N. Zadeh, C. D. Steenberg, J. S. Bois, B. R. Wolfe, M. B. Pierce, A. R. Khan, R. M. Dirks and N. A. Pierce, *J. Comput. Chem.*, 2011, **32**, 170–173.
- 42 W. M. Li, T. Bing, J. Y. Wei, Z. Z. Chen, D. H. Shangguan and J. Fang, *Biomaterials*, 2014, **35**, 6998–7007.

